

SCALABLE DECISION FOCUSED LEARNING VIA ON-LINE TRAINABLE SURROGATES

Anonymous authors

Paper under double-blind review

ABSTRACT

Decision support systems often rely on solving complex optimization problems that may require to estimate uncertain parameters beforehand. Recent studies have shown how using traditionally trained estimators for this task can lead to sub-optimal solutions. Using the actual decision cost as a loss function (called Decision Focused Learning) can address this issue, but with a severe loss of scalability at training time. To address this issue, we propose an acceleration method based on replacing costly loss function evaluations with an efficient surrogate. Unlike previously defined surrogates, our approach relies on unbiased estimators – reducing the risk of spurious local optima – and can provide information on its local confidence – allowing one to switch to a fallback method when needed. Furthermore, the surrogate is designed for a black-box setting, which enables compensating for simplifications in the optimization model and accounting for recourse actions during cost computation. In our results, the method reduces costly inner solver calls, with a solution quality comparable to other state-of-the-art techniques.

1 INTRODUCTION

Many real-world decision support systems, in domains such as logistics or production planning, rely on the solution of constrained optimization problems with parameters that are estimated via Machine Learning (ML) predictors. Literature from the last decade has showed how this approach, sometimes referred to as Prediction Focused Learning (PFL), can lead to poor decision quality due to a misalignment between the training objective (usually likelihood maximization) and the actual decision cost. Decision Focused Learning (DFL) (Amos & Kolter, 2017; Elmachtoub & Grigas, 2022) was then introduced to correct for this issue by training predictors for minimal decision regret.

While remarkable progress in the field has been made (Mandi et al., 2024), we argue that, **based on our experience with industrial optimization use cases**, three issues still prevent DFL from finding widespread practical application. First, **while DFL methods are very efficient at inference time**, their *training scalability is often severely limited*, since the problems encountered in decision support are frequently difficult (NP-hard or worse) and most DFL approaches require frequent solver calls and cost evaluations. Second, many DFL methods make *restrictive assumptions* on the decision problem (e.g. linear cost function, no parameters in the constraints); **in addition to limiting applicability, it has been shown (Hu et al., 2022; Elmachtoub et al., 2023) that such assumptions also cause the DFL advantage to vanish if the parameters expectations can be accurately estimated (appendix A)**. Third, several DFL methods require *explicit knowledge of the problem structure or the solver state*, which in a practical setting would require costly refactoring of the existing tools, or even a radical change of the solution technology. Solving these issues would allow one to use DFL for improving the effectiveness and robustness of *any real-world decision support tool*, while maintaining scalability.

We aim at making a significant step toward addressing these limitations, by relying on a carefully designed, efficient, surrogate to replace most solver calls at training time. **Our surrogate is suitable for a black-box setting, where no restrictive assumption is made on regret computation and no access to the solver state is needed**. Compared to the relevant state of the art: 1) our surrogate is an asymptotically unbiased regret estimator, i.e. with no irreducible approximation error; 2) we use a principled mechanism (stochastic smoothing and importance sampling) to address 0-gradients often occurring in DFL settings; 3) we include uncertainty quantification via a confidence level, used to decide when to dynamically update the surrogate based on samples generated by a fallback method.

054 Only a few of the existing DFL methods can be applied to achieve similar goals, a representative
 055 set of which is used as a baseline in our empirical evaluation. We design our experiments to assess
 056 the scalability and effectiveness of our method in a controlled setting, by comparing DFL and PFL
 057 on extended versions of standard benchmarks in the current literature. We emphasize problems
 058 with recourse actions and/or non-linearities, since they represent the settings where the benefits of
 059 DFL over PFL are robust even when accurate predictions can be obtained. We allow for scaling the
 060 problem complexity, to assess how the evaluated approaches behave on problems of different size
 061 (in terms of number of variables or parameters). In our results, our surrogate significantly reduces
 062 both the training runtime and the number of solver calls and cost evaluations. We also show that this
 063 acceleration, unlike previous attempts in the literature, does not adversely affect the decision quality,
 064 which remains comparable to other state-of-the-art techniques.

066 2 RELATED WORK

068 In the context of DFL problems where parameters are predicted by a machine learning model, initial
 069 works focused on implicit differentiation of the KKT conditions for optimality. In particular, Amos
 070 & Kolter (2017) handled convex quadratic programming, while Agrawal et al. (2019) extended it
 071 to conic programs. However, these initial methods were unsuitable for combinatorial problems,
 072 characterized by piecewise constant loss functions and uninformative gradients. Subsequent stud-
 073 ies such as Wilder et al. (2019); Mandi & Guns (2020) addressed MILP problems, by proposing
 074 to smooth the loss function through a regularization term (respectively L2 and log-barrier) com-
 075 puted over the decision variables. Other approaches introduced surrogate losses to overcome the
 076 zero-gradient problem. Elmachtoub & Grigas (2022) formalized the SPO+ loss as a regret upper
 077 bound, Mulamba et al. (2020) proposed the noise-contrastive estimation, Mandi et al. (2022) turned
 078 the problem into learning to rank on a pool of solutions. Many of these works also adopted a LP
 079 relaxation to speed up the training, which can however adversely affect the final solution quality, and
 080 it requires formulating the decision problem as a MILP. A surrogate loss, based on directional gradi-
 081 ents, is also proposed in Huang & Gupta (2024) and proved to provide unbiased gradient estimates,
 082 which allows it to outperform earlier approaches for strongly misspecified ML models. Unlike our
 083 approach, however, this method is restricted to problems with linear cost functions and is actually
 084 more computationally expensive at training time, due to the use of a zeroth-order gradient approx-
 085 imation. Finally, the approaches mentioned so far, with the exception of the KKT-based solutions,
 086 do not allow for predicted parameters appearing in the problem constraints. Attempts to cover the
 087 latter case include Paulus et al. (2021); Hu et al. (2023b;c;a), which require access to the problem
 formulation and either dedicated solvers or access to the solver internal state.

088 Only a few DFL approaches target the setting considered in this paper, where no assumption is
 089 made on the problem structure and training time scalability is emphasized; this is typically done by
 090 replacing the decision cost loss with fast-to-evaluate, differentiable, and learnable surrogates. The
 091 first studies in this class include Chung et al. (2022); Lawless & Zhou (2022), which used simple
 092 loss approximations with poor results. Recent advances are represented by the convex learnable
 093 surrogates proposed by Shah et al. (2022; 2024), and LANCER (Zharmagambetov et al., 2023),
 094 which employs a trainable neural network surrogate, fine-tuned at training time similarly to actor-
 095 critic approaches in reinforcement learning. These methods are closest to the one we propose, and
 096 differ mainly for their use of biased estimators and the lack of local confidence estimation.

097 DFL problems can also be formulated by treating the decision problem similarly to a reinforcement
 098 learning environment, as suggested by Silvestri et al. (2022). A notable example is the Score Func-
 099 tion Gradient Estimation (SFGE) method by Silvestri et al. (2023), inspired by Donti et al. (2017);
 100 Pogančić et al. (2019); Berthet et al. (2020); Mohamed et al. (2020) and Niepert et al. (2021), which
 101 combines stochastic smoothing and policy gradient methods. While we rely on Gaussian processes
 102 like Char et al. (2019), we use separate models and exploit contextual information via sample shar-
 103 ing, which simplifies the learning process and avoids length-scale and kernel issues.

105 3 PROBLEM FORMULATION

106 We consider a generalization of a DFL setting, where the parameters y of an optimization problem
 107 (e.g. demands) are not known at decision time, but can be estimated based on contextual informa-

tion x (e.g. hour of the day). Formally, let X and Y be random variables with support D_x and D_y , representing respectively contextual information and the uncertain parameters, and correlated according to their joint distribution $P(X, Y)$. At decision-making time, the problem parameters are estimated via a predictive model $h_\theta : D_x \rightarrow D_y$, with parameter vector θ . Based on the estimator output \hat{y} , we compute a decision vector z^* by solving a constrained optimization problem:

$$z^*(\hat{y}) = \arg \min_z \{f(\hat{y}, z) \mid z \in C(\hat{y})\} \quad (1)$$

where $f : D_y \times D_z \rightarrow \mathbb{R}$ is the problem cost function and $C : D_y \rightarrow 2^{D_z}$ is a constraint function that denotes the feasible space. We treat z^* as a function, assuming tie-breaking is used when multiple optimal solutions exist. Once the decisions are executed, their quality is determined by means of a second “true” cost function $g : D_y \times D_z \rightarrow \mathbb{R}$. Specifically, $g(y, z)$ represents the cost incurred by the solution z , under a realization y sampled from $P(Y \mid x)$.

The use of a distinct function g for decision quality evaluation distinguishes our setup from those typically used in DFL, and enables compensating for *misspecified decision problem models* – as opposed to misspecified predictors as in Huang & Gupta (2024). These can stem from treating uncertain parameters (e.g. travel times or demands) as deterministic, from disregarded minor constraints, or from approximated non-linearities – all common techniques to ensure scalability in real-world applications. This choice also allows us to deal with estimated parameters in the problem constraints in eq. (1), assuming that infeasible solutions can be repaired at an additional cost.

We wish to train h for minimal expected decision regret, approximated via a sample average:

$$\arg \min_\theta \frac{1}{m} \sum_{i=1}^m r(y_i, \hat{y}_i) \quad (2)$$

where $\{x_i, y_i\}_{i=1}^m \sim P(X, Y)$ is the training data, $\hat{y}_i = h_\theta(x_i)$ and $r(y_i, \hat{y}_i) = g(y_i, z^*(\hat{y}_i)) - g(y_i, z^*(y_i))$. Solving eq. (2) via first-order methods, as typically done with neural networks predictors, requires computing the gradient of the regret function, i.e.:

$$\frac{\partial}{\partial \theta} r(y_i, \hat{y}_i) = \frac{\partial g}{\partial z^*} \frac{\partial z^*}{\partial \hat{y}_i} \frac{\partial \hat{y}_i}{\partial \theta} \quad (3)$$

When the optimization problem is linear or combinatorial, or the g function is piecewise-constant, the gradient might be undefined or null on a large part of the predicted parameter space. Furthermore, evaluating the regret function requires computing z^* and g once per example and per training epoch, which can be prohibitively expensive, when the optimization problem is NP-hard, or the true cost function is based on optimization or simulation.

4 METHODOLOGY

We now introduce our method, whose main goal is accelerating the training problem of eq. (2). Similarly to Shah et al. (2022; 2024), we reduce the runtime by replacing, for every training example, the computationally heavy loss function $r(y_i, \hat{y})$ with a faster, trainable, surrogate loss $\tilde{r}_i(\hat{y})$. Formally, for a given realization y_i , associated to the i -th training example, the surrogate model is a function $\tilde{r}_i : D_y \rightarrow \mathbb{R}$ mapping a prediction vector \hat{y} into a corresponding loss value.

We identify three desirable properties for such a function. First, the surrogate should be *differentiable and have informative gradients everywhere*, to support gradient-descent optimization. Second, \tilde{r}_i should be capable of providing *unbiased gradient estimation* to ensure that, if enough calibration data is available, the local optima of the regret loss are preserved. The surrogate losses from Chung et al. (2022); Lawless & Zhou (2022); Shah et al. (2022; 2024) do not satisfy this criterion, running the risk of getting trapped in spurious local minima. Third, \tilde{r}_i should provide *confidence information* for online refinement; namely, one should be able to determine when the surrogate is reliable, and when instead a fallback method based on direct evaluation of z^* and g should be employed.

We propose using Gaussian Processes (GP) with Radial Basis Function (RBF) kernels for the surrogate, since they satisfy almost all the desired properties. In particular, GPs with RBFs are fully differentiable and can support efficient evaluation. Moreover, GPs are (asymptotically) unbiased estimators: given enough samples, they can approximate any function with arbitrarily high precision – though they are biased towards zero-centered predictions with scarce data. Finally, GPs have distributional output and naturally provide confidence information.

Stochastic smoothing The only property that GPs lack is tied to their nature as unbiased estimators. On the one hand, they are capable of accurately approximating the regret function; on the other hand, they risk inheriting some of its undesirable traits, such as 0 (or near-0) gradients on large swathes of the input space. One possible solution to this issue is to apply stochastic smoothing to the loss function – somewhat similarly to Silvestri et al. (2023). Specifically, our surrogate approximates a *smoothed* version of r_i , here called \bar{r}_i , referred to as $\bar{r}_i : D_y \rightarrow \mathbb{R}$ and defined as:

$$\bar{r}_i(\hat{y}) = \mathbb{E}_{\hat{y}' \sim \mathcal{N}(\hat{y}, \sigma)} [r_i(\hat{y}')] \quad (4)$$

The original loss value is replaced with its expectation under random, Normally distributed, perturbations of its input. The standard deviation σ is a controllable parameter in the method and represents the degree of smoothing. Small values of σ result in a more accurate regret approximation – at the cost of possibly weaker gradients – while higher σ values can provide more informative gradients – but may result in altered local optima. The effect of smoothing is depicted in fig. 1.

In principle, \bar{r}_i can be computed via a simple Monte Carlo approach. In practice, this is highly inefficient, because many samples would be needed for each input \hat{y} , and evaluating $r_i(\hat{y}')$ for each sample requires computing both z^* and g . We overcome this limitation by relying on importance sampling to perform multiple computations of $\bar{r}_i(\hat{y})$ based on the same set of observations. Formally, let $\{\hat{y}'_k\}_{k=1}^n$ be a set of predictions for which the value of $r_i(\hat{y}'_k)$ is known. We assume each of them has been sampled according to a distinct process, and refer to $\{q_k\}_{k=1}^n$ as the corresponding probabilities. These samples can be associated to an aggregated probability density function q , defined as a kernel density estimator, and used to define the importance weight function $w(\hat{y}, \hat{y}')$:

$$q(\hat{y}) = \frac{1}{n} \sum_{k=1}^n q_k(\hat{y}) \quad w(\hat{y}, \hat{y}') = \frac{\phi(\hat{y}'; \hat{y}, \sigma)}{q(\hat{y}')} \quad (5)$$

where $\phi(\cdot; \hat{y}, \sigma)$ is the density for a Normal distribution centered on \hat{y} and having standard deviation σ . Then we have:

$$\bar{r}_i(\hat{y}) \approx \sum_{k=1}^n \frac{w(\hat{y}, \hat{y}'_k)}{\sum_{h=1}^n w(\hat{y}, \hat{y}'_h)} r_i(\hat{y}'_k) \quad (6)$$

In practice, whenever a new prediction \hat{y}'_k is evaluated during the training process, we store both its regret value and the probability according to which it was sampled. **When training our GPs, we use as target the *smoothed* regret estimated via eq. (6).** This approach allows to increase the sampling efficiency and decrease the variance associated to the computation of \bar{r}_i ; at the same time it adds the flexibility to control the smoothing level by manipulating the sampling distributions. It is worth noting that, when a limited number of sampling points is available, the natural smoothing from the GPs combines with stochastic smoothing, leading to very regular landscapes for the surrogate loss. In fig. 1 we show an example of stochastic smoothing via importance sampling computed on a set of one-dimensional points sampled from Normal distributions.

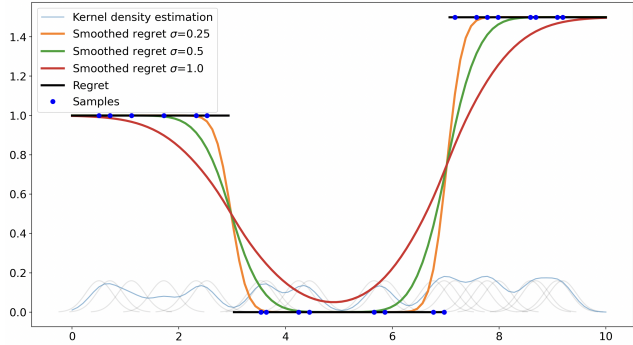
In Appendix B we discuss how stochastic smoothing affects our surrogate bias, and we show that our approach still has no irreducible error provide that abundant data is available and σ is small enough. In practice, higher σ values and few solver calls will be desirable, but the use of an expressive surrogate can decrease the risk of getting trapped in poor quality local optima.

Sample sharing Using a distinct surrogate for each training example permits unbiased regret estimation, at the same time limiting the number of input dimensions for the GPs. However, this also prevents information sharing among surrogates. With the aim to further reduce the number of r_i function evaluations, we devised an optional technique to enable sample sharing between different surrogates, if the corresponding regret landscapes are similar. Specifically, at the beginning of the training process, we perform Latin Hypercube Sampling (LHS) to collect a number points $\{\hat{y}_k\}_{k=1}^m$ in the prediction space D_y . We then associate each training example with a vector v containing the regret value computed for each such collected point, i.e. $v_i = \{r_i(\hat{y}_k)\}_{k=1}^m$. It can be seen that two samples i and j are associated to the same regret landscape iff:

$$\lim_{m \rightarrow \infty} \|v_i - v_j\|_2 = 0 \quad (7)$$

i.e., if the Euclidean distance between the corresponding vectors converges to 0, as the number of sampled points grows. Accordingly, we measure the similarity between the regret landscapes for

216
217
218
219
220
221
222
223
224
225
226
227



228
229
230
231

Figure 1: Illustration of stochastic smoothing with varying σ : larger values cause smoother functions with respect to the original regret loss. Smoothed functions are computed using importance sampling over a set of points sampled from Normal distributions.

232
233
234
235
236

two samples i and j in terms of such distance. It is worth noting that measuring distances on the contextual information space, as done by Shah et al. (2024), introduces a bias in the surrogates, since in a stochastic setting the same x input might be associated with different realizations and consequently with different loss landscapes.

237
238
239
240

We use the discussed similarity score to determine how relevant the data from one sample is for another sample. This is achieved by operating on the covariance matrix of each GP, by downscaling the kernel outputs. Specifically, let \hat{y}'_i and \hat{y}''_j be two predictions collected respectively for the training examples i and j ; then we have:

241
242

$$K_{new}(\hat{y}'_i, \hat{y}''_j) = \frac{K_{old}(\hat{y}'_i, \hat{y}''_j)}{1 + e^{\alpha \|v_i - v_j\|_2}} \quad (8)$$

243
244
245

where α is a learnable scale factor and the kernel value is unaltered if $i = j$, since the corresponding distance is 0. The collection phase required for this sample sharing process is also useful to initialize the set of GPs, and to perform standardization of the regret values that are used for their training.

246
247
248
249
250

It is worth noting that, in principle, using a single GP surrogate with access to the contextual input x , rather than one surrogate per example, would enable data sharing in a more natural fashion. Unfortunately, such a design choice would have a severe adverse effect on the surrogate scalability, as discussed in appendix C.

251
252
253

Algorithm We now dive into the concrete implementation of the main training procedure (see algorithm 1), starting from the outer training loop to solve eq. (2), and then moving to the inner training to optimize the GP surrogates.

254
255
256
257
258
259
260
261
262
263
264

Our surrogate loss should be combined with a fallback method, ideally one suitable for a general setting where no restrictive assumption on the regret function is made. One such example is the Score Function Gradient Estimation (SFGE) approach by Silvestri et al. (2023). Using this method has two additional benefits. First, SFGE also relies on stochastic smoothing, so that the set of predictions used for training the GPs can be naturally populated, their distribution of origin is known when computing $q(\hat{y})$, and the loss is semantically consistent between the surrogate and the fallback method. Second, the compound smoothing achieved by our GPs when few samples have been collected tends to compensate for the high variance and slow convergence of SFGE. That said, it should be possible to use our surrogate loss with a different fallback method, such as those from Hu et al. (2023a); Elmachtoub & Grigas (2022) or Huang & Gupta (2024). This investigation is left for future research.

265
266
267
268
269

The first step in algorithm 1 is a pretraining stage where we initialize the GPs and we collect pairs $(\hat{y}, r_i(\hat{y}))$ via LHS. We scale the number of points to be sampled logarithmically with respect to the dimensionality of D_y . We use these points to compute statistics to normalize the input \hat{y} (as GPs expect 0-mean input values) and to standardize the output $r_i(\hat{y})$. Then, for each training example, we employ the associated GP to compute a predicted mean and standard deviation. If the latter is below a threshold β (i.e., the GP is confident with respect to β), we take the mean as a surrogate loss

Algorithm 1 Training loop – gradient computation

```

270 gp ← initializeGPs(y)
271
272 for epoch in EPOCHS do
273     loss ← 0
274     i ← 0
275     while i < m do
276          $\hat{y}_i \leftarrow h_\theta(x_i)$ 
277          $\bar{r}_i, \sigma_i \leftarrow gp_i(\hat{y}_i)$ 
278         if  $\sigma_i < \beta$  then
279             loss ← loss +  $\bar{r}_i$ 
280         else
281              $q_i \leftarrow \mathcal{N}(\hat{y}_i, \sigma)$ 
282              $\hat{y}_i \sim q_i$ 
283             gp_i.add( $\hat{y}_i, r_i(\hat{y}_i), q_i$ )
284             loss ← loss + SFGE( $\hat{y}_i, r_i(\hat{y}_i), q_i$ )
285         i ← i + 1
286     gradient ← loss.backward()

```

and differentiate through the GP; otherwise, we call the SFGE procedure and we add the generated sample (and its generating distribution) to the corresponding GP. We aggregate loss terms for each training instance into a single loss, mixing values from the surrogates and the fallback method, before gradient computation.

We trigger surrogate training when at least t new sample-target pairs are available. New data points are then shared between similar GPs, if such option is enabled, according to a maximum tolerable Euclidean distance d_{max} . We replace the $r_i(\hat{y})$ targets with the smoothed ones $\bar{r}_i(\hat{y})$, using eq. (6) on the collected samples and distributions. We also apply data preprocessing by normalizing the inputs and standardizing the outputs, on the basis of the statistical information extracted in the pretraining phase. We train GPs by maximum likelihood estimation, with a classical RBF kernel and a length-scale prior $l_i \sim \text{LogNormal}(\log(\dim(Y))/2, 1)$. We add this last regularization term, following Hvarfner et al. (2024), to improve scalability in higher dimensions. Finally, the RBF kernels are warm-started in all subsequent trainings, so as to speed up their training. The code for our method is publicly available at `currently-in-the-supplemental-material`.

5 EXPERIMENTS

We now discuss the experimental analysis conducted to assess the robustness, reliability, accuracy, and especially scalability of our method. We designed experiments to answer four main research questions. **Q1.** How does our surrogate loss perform in terms of decision quality compared to the relevant baselines? **Q2.** How many calls to the black-box solver does it require? **Q3.** How much runtime does it take to converge compared to the other methods? **Q4.** Can it be scaled to high dimensions?

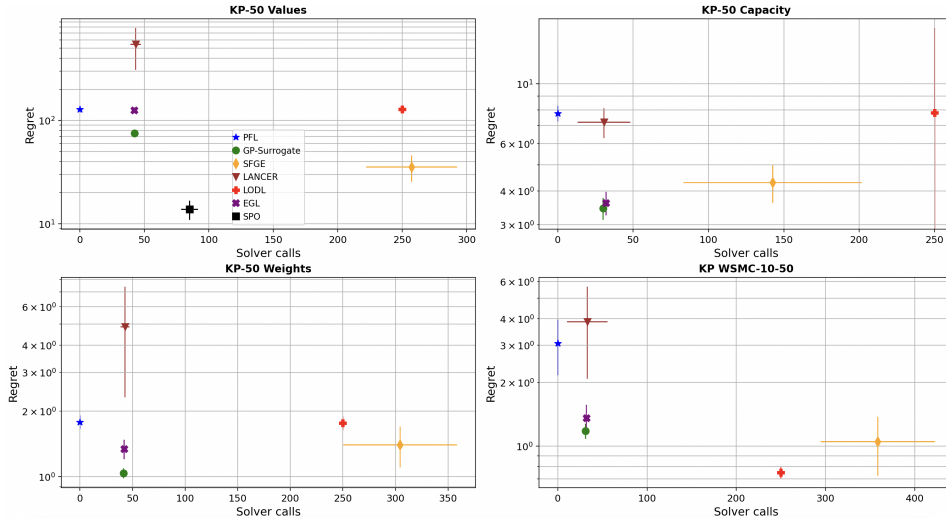
Benchmarks We consider three problem classes, many of which include recourse actions to repair violated constraints, thus leading to misspecified, realistic, decision problems.

Knapsack (KP). We generate 1-0 KP datasets following the procedure proposed by Elmachtoub & Grigas (2022) to model a stochastic mapping between input features x and ground-truth targets y , with a polynomial degree $deg = 5$, number of input features $dim(X) = 5$, a noise half-width $\bar{\epsilon} = 0.5$, and a Poisson distribution to correlate x and y . In our experiments we build datasets on a target space of $dim(Y) = 50$ items. We make use of three different setups, respectively injecting uncertainty (i.e., stochastic correlation) into weights, values and capacity. We also adopt the recourse action system by Silvestri et al. (2023), with a fixed penalty $p = 10$.

Weighted Set Multi-Cover (WSMC). We create WSMC datasets with $dim(X) = 5$ input features, $dim(Y) = 10$ items and $s = 50$ sets, following the guidelines by Grossman & Wool (1997) to generate realistic availability matrices and the same stochastic correlation as in Elmachtoub & Grigas (2022). We use the recourse action adopted by Silvestri et al. (2023), with a fixed penalty $p = 10$.

324 *Toy.* We define a synthetic toy dataset. In this setting the input features are deterministically mapped
 325 to a target space, using a weight matrix $W \in R^{dim(Y) \times dim(X)} \sim U(0, 1)$, such that $y = Wx$.
 326 The underlining optimization problem is a trivial map where $z^*(\hat{y}) = \hat{y}$, while the cost is given by
 327 a pseudoconvex piecewise step function with minimum in y : $g(y, z^*(\hat{y})) = s \lfloor \|y - \hat{y}\|_2 / l \rfloor$, where s
 328 controls the step heights and l determines the distance between steps. We set $s = 5$ and $l = 1$ in our
 329 experiments. This new benchmark provides a controlled way to investigate convergence properties,
 330 as the entire loss landscape is known. Additionally, it allows for changing the dimensionality of Y ,
 331 while keeping a negligible cost for computing z^* , so to stress DFL techniques on larger scales.
 332

333 **Baselines** Our baselines include a predictive model trained for maximum likelihood, referred to as
 334 Prediction Focused Learning (PFL), plus state-of-the-art DFL methods that apply to black-box set-
 335 tings. In particular, we include in our comparison the SFGE method by Silvestri et al. (2023), which
 336 also serves as fallback for our approach, allowing us to directly assess the impact of the surrogate-
 337 based acceleration. For this method, we use a trainable parameter for σ , with starting value 0.1,
 338 and we warm start the predictor via PFL training. We then consider EGL, LODL, and LANCER,
 339 respectively from Shah et al. (2024), Shah et al. (2022) and Zharmagambetov et al. (2023), as rep-
 340 resentative of other state-of-the-art black-box surrogate-based approaches. We employ the same set
 341 of hyperparameters proposed by the authors, implementing all the four convex surrogates (MSE,
 342 Directed-MSE, Quadratic, Directed-Quadratic) and fixing the number of samples to 250 for LODL
 343 and to 32 or 42 for EGL, to put it on par with our model in terms of calls, for a fair regret compar-
 344 ison. We adopt the same surrogate model architecture proposed in Zharmagambetov et al. (2023) for
 345 LANCER, with two hidden layers of 200 units and tanh activation functions; we set $t = 10$ for the
 346 dual training. As a representative of a state-of-the-art DFL method requiring restrictive assumptions,
 347 we include SPO+ by Elmachtoub & Grigas (2022), where applicable.
 348



357
 358
 359
 360
 361
 362
 363
 364
 365
 366
 367
 368
 369
 370
 371
 372
 373
 374
 375
 376
 377

Figure 2: Regret and solver calls across the benchmarks: points represent the average regret (on a logarithmic scale) and average solver calls per instance for all the baselines. Lines represent standard deviations for each method. Only the best (lowest regret) models are reported for LODL and EGL.

369 **Results** In this section we report results on a set of experiments designed to answer the discussed
 370 research questions. For each setting we generate 5 datasets, each one containing 1000 instances,
 371 differently split into train (80%), validation (10%) and test sets (10%). All the models are trained
 372 with the Adam algorithm by Kingma (2014) and a learning rate $lr = 10^{-3}$, using an early stop-
 373 ping criterion on regrets computed on the validation set, to avoid overfitting. We enable stochastic
 374 smoothing, differentiation, and pretraining for our method, here named GP-Surrogate. By default,
 375 we keep sample sharing off, as it is best suited to improve speed on very time-consuming problems,
 376 at the cost of solution quality (see table 3 for more details). We set $\beta = 1.0$ as a tradeoff between
 377 speed and precision in learning, as shown in appendix F, and $t = 40$. All the experiments were run
 on an Apple M3 Pro CPU with 12 cores and 18GB of RAM.

Table 1: Runtime and average regret for GP-Surrogate and SFGE on WSMC-10 with 250, 500, 750 and 1000 sets. Time limit is 900s.

	<i>Method</i>	<i>WSMC-10-250</i>	<i>WSMC-10-500</i>	<i>WSMC-10-750</i>	<i>WSMC-10-1000</i>
<i>Runtime</i>	GP-Surrogate	289.24 ± 6.54	459.70 ± 15.73	638.50 ± 14.70	818.44 ± 17.74
	SFGE	900.0* ± 0.0	900.0* ± 0.0	900.0* ± 0.0	900.0* ± 0.0
<i>Regret</i>	GP-Surrogate	1.55 ± 0.57	1.51 ± 0.50	1.48 ± 0.54	1.51 ± 0.59
	SFGE	1.83 ± 0.86	2.44 ± 1.05	2.82 ± 1.20	3.54 ± 1.25

Q1. We compare the regret for each approach on the KP with 50 items (KP-50) and uncertainty in weights, values and capacity, and on the the WSMC with 10 items and 50 sets (WSMC-10-50). Results, summarized in fig. 2 and presented in extended form in appendix D, indicate that using our surrogate on top of SFGE leads to solutions of similar quality (or even better) in all but one benchmark, and with less variability. GP-Surrogate provides better regret and stability than the best approaches in the LODL and EGL class. We also found the performance of LODL and EGL to be inconsistent w.r.t. the employed convex surrogate, as highlighted in appendix D. Overall, our method seems to provide a better alternative for accelerating training than these approaches, at least in terms of regret, most likely thanks to its lack of a structural estimation bias, and to the ability to switch to the fallback method in case of low confidence. The surrogate model used by LANCER seems often unable to reasonably approximate the real loss landscape, causing inconsistent training results and high regrets (even more than PFL), despite a significant reduction in terms of solver calls. The SPO method, when applicable, significantly outperforms all the others, which suggests that traditional DFL approaches should still be preferred to black-box ones when permitted by their assumptions.

Q2. We adopt the same datasets as in Q1 to analyze the computational cost of all approaches. Results are again depicted in fig. 2. In appendix E we report the number of solver calls (per training sample), and the total runtime for each method. The former metric should be considered more important, as for any sufficiently difficult problem the decision time will be the dominant factor. GP-Surrogate reduces the number of calls by almost an order of magnitude compared to its fallback method, greatly increasing viability in a practical setting. We align the number of EGL samples to the solver calls from our method and observe EGL performing significantly worse in terms of regret. The LODL approaches, in their reference configuration, perform more solver calls for even worse regret in all but one benchmark. The same considerations apply for the runtime.

Q3. We evaluate scalability for complex problems with time-consuming solver calls, by building versions of the WSMC-10 datasets with an increasing number of item sets. For this experiment we set a time limit of 900s per training attempt, to simulate real-world scenarios with limited computational resources. We compare GP-Surrogate with SFGE and report the results in table 1. As it can be seen, GP-Surrogate consistently achieves training convergence. SFGE fails to do so even in the simplest cases, which causes the approach to have worse regret than GP-Surrogate in this case.

Q4. We evaluate scalability for high-dimensional predictions (as opposed to larger-size problems like in Q3), by increasing the number of decision variables in the Toy benchmark. We report results in table 2. SFGE gets stuck into local optima, likely because of the nature of this synthetic problem, which requires strong variations of σ across the training steps. Conversely, GP-Surrogate is still able to effectively minimize the loss function. This behavior shows that our surrogates can enable convergence to high-quality solutions, even in high-dimensional spaces. We conjecture this is partly due to the fact that, since the realization y is always used when training the GPs, they can naturally identify the presence of a local minimum for r_i at that location; this property is shared with the surrogates from Shah et al. (2022), but with all the discussed benefits of our solution.

Overall, the experiments indicate that our approach can outperform its fallback method in terms of solver calls and total runtime, thus making it scalable to complex problems, while keeping a comparable and sometimes better decision quality. The degree of acceleration is similar to the LODL, EGL, and LANCER models, but with improved consistency, reliability, and solution quality. Finally, the method scales much better than SFGE on high-dimensional parameter spaces, thanks to the combination of stochastic and GP smoothing.

Table 2: Average regret for GP-Surrogate and SFGE on the Toy dataset with 64, 128, 256 and 512 dimensions.

	<i>Method</i>	<i>Toy-64</i>	<i>Toy-128</i>	<i>Toy-256</i>	<i>Toy-512</i>
<i>Regret</i>	GP-Surrogate	5.61 ± 2.97	4.18 ± 0.96	1.29 ± 0.46	0.29 ± 0.23
	SFGE	39.78 ± 3.06	58.61 ± 1.02	113.28 ± 3.41	271.82 ± 9.49

Table 3: Average regret and average calls per instance for GP-Surrogate with different components on KP-50 with uncertain weights, values and capacity and WSMC-10 with 50 sets.

	<i>Method</i>	<i>KP-50 weights</i>	<i>KP-50 values</i>	<i>KP-50 capacity</i>	<i>WSMC-10-50</i>
<i>Regret</i>	FULL MODEL	1.14 ± 0.11	106.38 ± 10.19	3.52 ± 0.33	1.39 ± 0.23
	SMOOTHING OFF	1.40 ± 0.11	149.67 ± 16.68	3.64 ± 0.52	1.42 ± 0.19
	PRETRAIN OFF	1.15 ± 0.08	57.83 ± 2.61	5.04 ± 0.33	0.67 ± 0.10
	SAMPLE SHARING OFF	1.04 ± 0.05	75.07 ± 5.20	3.45 ± 0.31	1.18 ± 0.09
	DIFFERENTIATION OFF	1.63 ± 0.21	156.56 ± 25.23	3.61 ± 0.57	1.58 ± 0.71
<i>St. calls</i>	FULL MODEL	39.84 ± 2.51	35.41 ± 0.48	6.93 ± 0.14	28.31 ± 1.10
	SMOOTHING OFF	41.58 ± 0.74	36.44 ± 0.35	6.97 ± 0.12	29.20 ± 0.59
	PRETRAIN OFF	121.71 ± 3.71	88.34 ± 2.55	48.91 ± 0.60	72.65 ± 9.41
	SAMPLE SHARING OFF	41.33 ± 1.22	42.32 ± 0.09	30.04 ± 0.05	31.06 ± 0.35
	DIFFERENTIATION OFF	42.40 ± 4.69	36.28 ± 0.48	6.95 ± 0.15	28.95 ± 1.03

Ablation studies To prove the effectiveness of all the major components of our method, we also conducted an ablation study by separately disabling stochastic smoothing, pretraining, sample sharing and GP differentiation. Results, reported in table 3, reveal that in all the settings removing differentiation or smoothing causes higher average regrets and solver calls, highlighting their relevance. Results with no sample sharing are the same of fig. 2; we note that sharing points between GP models affects negatively the average regrets, but reduces the average calls. In most cases, this extra source of acceleration is not enough to justify the lower decision quality, but it can be extremely valuable in some cases, as observed in the KP-50 capacity benchmark where the number of solver call is almost two orders of magnitude lower than SFGE. For what concerns pretraining, the number of solver calls grows sensibly when it is turned off, proving its fundamental role for learning confident surrogates in early stages. However, relying more on the fallback method does not imply a downgrade in terms of regrets; in fact, in two settings out of four, we see a strong improvement when the surrogate usage is more moderate.

6 CONCLUSIONS

We present an approach to improve the applicability of DFL methods, targeting scenarios where solution and cost computation are time-consuming and where access to the problem structure and solver state is impossible or inconvenient. In this setting, the existing DFL approaches are too slow to converge, they may not be applicable, or they accelerate the training process at the cost of a worse decision quality. We employ a GP-based surrogate loss function, trained online in alternation with a fallback method, to exploit the surrogate speed without losing the ability to adapt to the regret function landscape. We solve the 0-gradient issue relying on stochastic smoothing via importance sampling – which also motivates our choice of SFGE for the fallback method. Our experimental evaluation reveals that our surrogate matches or outperforms SFGE, while reducing the number of solver calls by up to two orders of magnitude, depending on the problem and the model configuration. Our method improves over related approaches in terms of sample efficiency, solution quality, or both. Finally, we show that the approach can be scaled to higher dimensions. Some potential directions of improvement remain unexplored. A point of particular interest is the possibility to adjust the smoothing factor, or the points where smoothed regret is computed, at training time – without the need to collect additional samples. Moreover, by adapting acquisition functions from classical Bayesian optimization, it might be possible to remove the need for a fallback method. Finally, similar to the LODL, EGL, and LANCER approaches, our learned surrogates could be exported for the construction of new training sets or generally for approximating regret evaluation.

486 REPRODUCIBILITY CHECKLIST

487
488 Based on the AAAI format:

- 489 • Includes a conceptual outline and/or pseudocode description of AI methods introduced: **yes**
- 490 • Clearly delineates statements that are opinions, hypothesis, and speculation from objective
- 491 facts and results: **yes**
- 492 • Provides well-marked pedagogical references for less-familiar readers to gain background
- 493 necessary to replicate the paper: **yes**
- 494 • A motivation is given for why the experiments are conducted on the selected datasets: **yes**
- 495 • All datasets drawn from the existing literature (potentially including authors' own previ-
- 496 ously published work) are publicly available: **yes**
- 497 • This paper states the number and range of values tried per (hyper-) parameter during devel-
- 498 opment of the paper, along with the criterion used for selecting the final parameter setting:
- 499 **partial**
- 500 • Any code required for pre-processing data is included in the appendix: **yes**
- 501 • All source code required for conducting and analyzing the experiments is included in a
- 502 code appendix: **yes**
- 503 • All source code required for conducting and analyzing the experiments will be made pub-
- 504 ically available upon publication of the paper with a license that allows free usage for re-
- 505 search purposes: **yes**
- 506 • All source code implementing new methods have comments detailing the implementation,
- 507 with references to the paper where each step comes from: **partial**
- 508 • If an algorithm depends on randomness, then the method used for setting seeds is described
- 509 in a way sufficient to allow replication of results: **yes**
- 510 • This paper specifies the computing infrastructure used for running experiments (hardware
- 511 and software), including GPU/CPU models; amount of memory; operating system; names
- 512 and versions of relevant software libraries and frameworks: **partial**
- 513 • This paper formally describes evaluation metrics used and explains the motivation for
- 514 choosing these metrics: **yes**
- 515 • This paper states the number of algorithm runs used to compute each reported result: **yes**
- 516 • Analysis of experiments goes beyond single-dimensional summaries of performance (e.g.,
- 517 average; median) to include measures of variation, confidence, or other distributional in-
- 518 formation: **yes**
- 519 • The significance of any improvement or decrease in performance is judged using appropri-
- 520 ate statistical tests (e.g., Wilcoxon signed-rank): **no**
- 521 • This paper lists all final (hyper-)parameters used for each model/algorithm in the paper's
- 522 experiments: **yes**
- 523
- 524
- 525
- 526

527 REFERENCES

- 528 Akshay Agrawal, Brandon Amos, Shane Barratt, Stephen Boyd, Steven Diamond, and J Zico Kolter.
529 Differentiable convex optimization layers. *Advances in neural information processing systems*,
530 32, 2019.
- 531
- 532 Brandon Amos and J Zico Kolter. Optnet: Differentiable optimization as a layer in neural networks.
533 In *International conference on machine learning*, pp. 136–145. PMLR, 2017.
- 534
- 535 Quentin Berthet, Mathieu Blondel, Olivier Teboul, Marco Cuturi, Jean-Philippe Vert, and Francis
536 Bach. Learning with differentiable pertubed optimizers. *Advances in neural information process-*
537 *ing systems*, 33:9508–9519, 2020.
- 538
- 539 Ian Char, Youngseog Chung, Willie Neiswanger, Kirthevasan Kandasamy, Andrew O Nelson, Mark
Boyer, Egemen Kolemen, and Jeff Schneider. Offline contextual bayesian optimization. *Advances*
in Neural Information Processing Systems, 32, 2019.

- 540 Tsai-Hsuan Chung, Vahid Rostami, Hamsa Bastani, and Osbert Bastani. Decision-aware learning
541 for optimizing health supply chains. *arXiv preprint arXiv:2211.08507*, 2022.
- 542 Priya Donti, Brandon Amos, and J Zico Kolter. Task-based end-to-end model learning in stochastic
543 optimization. *Advances in neural information processing systems*, 30, 2017.
- 544 Adam N Elmachtoub and Paul Grigas. Smart “predict, then optimize”. *Management Science*, 68(1):
545 9–26, 2022.
- 546 Adam N Elmachtoub, Henry Lam, Haofeng Zhang, and Yunfan Zhao. Estimate-then-optimize ver-
547 sus integrated-estimation-optimization versus sample average approximation: a stochastic domi-
548 nance perspective. *arXiv preprint arXiv:2304.06833*, 2023.
- 549 Tal Grossman and Avishai Wool. Computational experience with approximation algorithms for the
550 set covering problem. *European journal of operational research*, 101(1):81–92, 1997.
- 551 Xinyi Hu, Jasper Lee, and Jimmy Lee. Two-stage predict+ optimize for milps with unknown pa-
552 rameters in constraints. *Advances in Neural Information Processing Systems*, 36:14247–14272,
553 2023a.
- 554 Xinyi Hu, Jasper CH Lee, and Jimmy HM Lee. Branch & learn with post-hoc correction for pre-
555 dict+ optimize with unknown parameters in constraints. In *International Conference on Integra-
556 tion of Constraint Programming, Artificial Intelligence, and Operations Research*, pp. 264–280.
557 Springer, 2023b.
- 558 Xinyi Hu, Jasper CH Lee, and Jimmy HM Lee. Predict+ optimize for packing and covering lps
559 with unknown parameters in constraints. In *Proceedings of the AAAI Conference on Artificial
560 Intelligence*, volume 37, pp. 3987–3995, 2023c.
- 561 Yichun Hu, Nathan Kallus, and Xiaojie Mao. Fast rates for contextual linear optimization. *Manage-
562 ment Science*, 68(6):4236–4245, 2022.
- 563 Michael Huang and Vishal Gupta. Decision-focused learning with directional gradients. *Advances
564 in Neural Information Processing Systems*, 37:79194–79220, 2024.
- 565 Carl Hvarfner, Erik Orm Hellsten, and Luigi Nardi. Vanilla bayesian optimization performs great in
566 high dimensions. *arXiv preprint arXiv:2402.02229*, 2024.
- 567 Diederik P Kingma. Adam: A method for stochastic optimization. *arXiv preprint arXiv:1412.6980*,
568 2014.
- 569 Connor Lawless and Angela Zhou. A note on task-aware loss via reweighing prediction loss by
570 decision-regret. *arXiv preprint arXiv:2211.05116*, 2022.
- 571 Jayanta Mandi and Tias Guns. Interior point solving for lp-based prediction+ optimisation. *Advances
572 in Neural Information Processing Systems*, 33:7272–7282, 2020.
- 573 Jayanta Mandi, Victor Bucarey, Maxime Mulamba Ke Tchomba, and Tias Guns. Decision-focused
574 learning: Through the lens of learning to rank. In *International conference on machine learning*,
575 pp. 14935–14947. PMLR, 2022.
- 576 Jayanta Mandi, James Kotary, Senne Berden, Maxime Mulamba, Victor Bucarey, Tias Guns, and
577 Ferdinando Fioretto. Decision-focused learning: Foundations, state of the art, benchmark and
578 future opportunities. *Journal of Artificial Intelligence Research*, 80:1623–1701, 2024.
- 579 Shakir Mohamed, Mihaela Rosca, Michael Figurnov, and Andriy Mnih. Monte carlo gradient esti-
580 mation in machine learning. *Journal of Machine Learning Research*, 21(132):1–62, 2020.
- 581 Maxime Mulamba, Jayanta Mandi, Michelangelo Diligenti, Michele Lombardi, Victor Bucarey, and
582 Tias Guns. Contrastive losses and solution caching for predict-and-optimize. *arXiv preprint
583 arXiv:2011.05354*, 2020.
- 584 Mathias Niepert, Pasquale Minervini, and Luca Franceschi. Implicit mle: backpropagating through
585 discrete exponential family distributions. *Advances in Neural Information Processing Systems*,
586 34:14567–14579, 2021.

594 Anselm Paulus, Michal Rolínek, Vít Musil, Brandon Amos, and Georg Martius. Comboptnet: Fit the
595 right np-hard problem by learning integer programming constraints. In *International Conference*
596 *on Machine Learning*, pp. 8443–8453. PMLR, 2021.

597
598 Marin Vlastelica Pogančić, Anselm Paulus, Vit Musil, Georg Martius, and Michal Rolinek. Differ-
599 entiation of blackbox combinatorial solvers. In *International Conference on Learning Representations*, 2019.
600

601 Sanket Shah, Kai Wang, Bryan Wilder, Andrew Perrault, and Milind Tambe. Decision-focused
602 learning without decision-making: Learning locally optimized decision losses. *Advances in Neu-*
603 *ral Information Processing Systems*, 35:1320–1332, 2022.

604
605 Sanket Shah, Bryan Wilder, Andrew Perrault, and Milind Tambe. Leaving the nest: Going beyond
606 local loss functions for predict-then-optimize. In *Proceedings of the AAAI Conference on Artificial*
607 *Intelligence*, volume 38, pp. 14902–14909, 2024.

608
609 Mattia Silvestri, Allegra De Filippo, Michele Lombardi, and Michela Milano. Unify: a unified pol-
610 icy designing framework for solving constrained optimization problems with machine learning.
arXiv preprint arXiv:2210.14030, 2022.

611
612 Mattia Silvestri, Senne Berden, Jayanta Mandi, Ali İrfan Mahmutoğulları, Brandon Amos, Tias
613 Guns, and Michele Lombardi. Score function gradient estimation to widen the applicability of
614 decision-focused learning. *arXiv preprint arXiv:2307.05213*, 2023.

615
616 Bryan Wilder, Bistra Dilkina, and Milind Tambe. Melding the data-decisions pipeline: Decision-
617 focused learning for combinatorial optimization. In *Proceedings of the AAAI Conference on*
Artificial Intelligence, volume 33, pp. 1658–1665, 2019.

618
619 Arman Zharmagambetov, Brandon Amos, Aaron Ferber, Taoan Huang, Bistra Dilkina, and Yuan-
620 dong Tian. Landscape surrogate: Learning decision losses for mathematical optimization under
621 partial information. *Advances in Neural Information Processing Systems*, 36:27332–27350, 2023.
622
623
624
625
626
627
628
629
630
631
632
633
634
635
636
637
638
639
640
641
642
643
644
645
646
647

A CONDITIONS FOR THE EFFECTIVENESS OF THE CLASSICAL DFL SETTING

Most classical Decision Focused Learning approaches focus on the following setting:

$$\arg \min_{\theta} \mathbb{E}_{x,y \sim P(X,Y)} [r(y, \hat{y})] \quad (9)$$

where we have:

$$r(y, \hat{y}) = y^T z^*(\hat{y}) - y^T z^*(y) \quad (10)$$

$$z^*(\hat{y}) = \arg \min_z \{\hat{y}^T z \mid z \in C\} \quad (11)$$

This “classical” setting differs from the one described in this paper in three key respects:

1. The considered optimization problem has a linear cost function and a constraint set that does not depend on the uncertain parameters
2. The uncertain parameters correspond to the coefficients of the linear cost function
3. The true cost function (g in our setup) is the same as that used in the optimization problem, i.e. eq. (10) and eq. (11) use the same cost function

The assumptions in the classical setup are used by state of the art DFL methods to obtain good convergence speed and excellent solution quality. However, the same assumptions also introduce some notable limitations.

We start by observing that, since the $y^T z^*(y)$ term in the regret expression does not depend on the predictions, we have that:

$$\arg \min_{\theta} \mathbb{E}_{x,y \sim P(X,Y)} [r(y, \hat{y})] = \arg \min_{\theta} \mathbb{E}_{x,y \sim P(X,Y)} [y^T z^*(\hat{y})] \quad (12)$$

A similar equivalence holds for all DFL settings, including the one we consider. In the classical DFL setting, however, the linearity of the cost function also implies that:

$$\arg \min_{\theta} \mathbb{E}_{x,y \sim P(X,Y)} [y^T z^*(\hat{y})] = \arg \min_{\theta} \mathbb{E}_{x \sim P(X)} [\mathbb{E}_{y \sim P(Y|x)} [y]^T z^*(\hat{y})] \quad (13)$$

It can be seen that an optimal solution for eq. (13) can be obtained by setting $\hat{y} = \mathbb{E}_{x,y \sim P(X,Y)} [y]$, i.e. if the ML predictor provides a correct estimate of the expectation of the uncertain parameters.

In practical terms, this means that, in the classical setting, *the advantage of DFL over PFL becomes vanishingly small, unless the ML predictor has an irreducible estimation error*, i.e. it is misaligned – see for example Huang & Gupta (2024). DFL methods can still be useful, for example when the correct distribution $P(Y | X)$ is not known, or when a simpler ML model (e.g. a linear regressor) is desirable for easier analysis. However, this weakness significantly reduces the practical appeal of the classical DFL setting.

The reduction from eq. (12) does not apply in general to our black-box setting, which makes our approach capable of addressing stochastic problems with non-linear costs and/or recourse action, on which the advantage provided by DFL can be robust, regardless of the predictor expressivity.

B ESTIMATION BIAS ANALYSIS

One of the appeals of our proposed approach is that it relies on surrogates that can provide an unbiased estimation of the regret. While this claim is limited to the abundant data regime, it is still relevant since it implies that our approach does not introduce an irreducible error in the regret estimation. Here, we proceed to detail our claim and provide a proof sketch.

Consider the DFL training problem as stated in eq. (2), and its variant defined over our proposed surrogates, i.e.:

$$\arg \min_{\theta} \frac{1}{m} \sum_{i=1}^m \tilde{r}_i(\hat{y}) \quad (14)$$

The loss functions employed in the two cases are separable over the training examples. As a consequence, one can see that as long as the surrogate $\tilde{r}_i(\hat{y}_i)$ can provide an arbitrarily accurate approximation of the true regret $r(y_i, \hat{y}_i)$ for every input point, then the surrogate loss is also an arbitrary accurate approximation of the true loss. Formally, we have that:

$$\forall i = 1..m, \hat{y}_i \in D_y, \tilde{r}_i(\hat{y}_i) \simeq r(y_i, \hat{y}_i) \implies \forall \hat{y}_i \in D_y, \sum_{i=1}^m \tilde{r}_i(\hat{y}_i) \simeq \sum_{i=1}^m r(y_i, \hat{y}_i) \quad (15)$$

By relying on linearity of differentiation operator and on universal quantification over the regret input, we get an analogous result for the loss gradient:

$$\forall i = 1..m, \hat{y}_i \in D_y, \tilde{r}_i(\hat{y}_i) \simeq r(y_i, \hat{y}_i) \implies \forall \hat{y}_i \in D_y, \nabla_{\theta} \sum_{i=1}^m \tilde{r}_i(\hat{y}_i) \simeq \nabla_{\theta} \sum_{i=1}^m r(y_i, \hat{y}_i) \quad (16)$$

which can be proved by relying on the definition of partial derivative as the limit for a finite difference. Therefore, as long as each surrogate $\tilde{r}_i(\hat{y}_i)$ can approximate sufficiently well the regret landscape for the corresponding training example, then our surrogate loss accurately approximates the true DFL loss and its gradient accurately approximates the true gradient.

Now, it can be seen the true regret $r(y_i, \hat{y}_i)$ is a deterministic function of \hat{y}_i , since it refers to a specific realization of the random variable Y . Assuming arbitrarily abundant, uniformly sampled, values of \hat{y}_i , a Gaussian Process with an RBF kernel can approximate any deterministic function with an approximation error that converges to 0 as the number of datapoints used for training the GP grows. If the regret landscape $r(y_i, \hat{y}_i)$ is smooth, then the approximation error can reach 0; for the kind of discontinuous, piecewise constant, regret landscapes that we are primarily interested in, the approximation error approaches 0^+ rather than 0, which is sufficient for our purpose.

In our approach, the GP surrogates are trained to approximate the smoothed regret $\bar{r}_i(\hat{y})$, rather than the true regret. We will show that, under some conditions, this can still result in an arbitrarily accurate estimate of the true regret, in the sense that the approximation error can approach 0^+ . First, observe that, in the same abundant data regime considered before and for a centered smoothing distribution (such as a the Normal distribution we use), the expectation used in stochastic smoothing will be estimated to arbitrarily accurate precision by a sample average. Second, for a sufficiently low value of σ the Normal distribution will converge to a Dirac delta, and as a consequence:

$$|\bar{r}_i(\hat{y}) - r(y_i, \hat{y}_i)| \xrightarrow{\sigma \rightarrow 0^+} 0^+ \quad (17)$$

Therefore, an arbitrarily accurate estimate of the true regret can be obtained by lowering the smoothing factor σ .

Overall, we have that: 1) for abundant data points sampled uniformly at random; and 2) for a sufficiently low smoothing factor σ , our surrogates can provide an arbitrarily accurate approximation of the true regret.

From a practical point of view, using abundant samples runs counter to our main goal of improving scalability, and using larger values of σ will typically provide more informative gradient. The result we have just proved is however significant since it means our surrogate *does not suffer from an irreducible approximation error*, unlike other approaches from the literature such as LODL or EGL.

C SCALABILITY CONSIDERATIONS

Due to the complexity of the DFL pipeline, there are different terms that can affect scalability. Those include:

- The number M of training examples
- The number H of training epochs
- The number m_i of datapoints (prediction-regret pairs) used to train the GP surrogate for the i -th example
- The number n_y of predicted parameters appearing in the optimization model (and representing the input of our GP surrogates)

- The number n_x of components in the contextual information vector

Since our focus is on improving training time scalability, we can expect that, in a practical situation:

- The number of parameters n_y should be relatively small, since the optimization problem being solved will likely have NP-hard or high-degree polynomial complexity
- The number of datapoints m_i for each example should be quite small, and in particular much smaller than the number of epochs H , otherwise using only the fallback method would be better

The number of examples M , of training epochs H , and of components n_x in the contextual information vector can be large in general.

We can now observe that:

- Since we learn a separate GP per example, the computational cost for our surrogates scales as $O(M)$ with respect to the number of examples
- The cost for computing the covariance matrices used by each GP scales as $O(n_y m_i^2)$, since it requires $O(m_i^2)$ kernel computations, each running in $O(n_y)$. As stated above, both n_y and m_i can be expected to be small in practice
- The cost for training (and re-training) the GP surrogates via gradient descent can be expected to scale as $O(H)$ with respect to the number of epochs

Our sample sharing mechanism, if enabled, complicates the picture, by virtually increasing the number m_i of datapoints used to training every GP. However, since we use a distance cutoff for including shared samples, we observed only a modest increase in our experiments.

Overall, our design ensures that all higher-degree polynomial complexity terms are computed over low-dimensional objects, thus keeping the method quite scalable.

Notice that using a single surrogate model using pairs (x, \hat{y}) as input – a seemingly more natural choice – would allow to directly train the model over all collected datapoints, but would also make the covariance computation scale as $O((n_x + n_y)(m_i M)^2)$, which would be prohibitively expensive.

D EXTENDED RESULTS

We report in table 4 complete results relative to the average regret score for all the models, including all the LODL and EGL variations.

Table 4: Average regret for all the models on KP-50 with uncertain weights, values and capacity and WSMC-10 with 50 sets.

<i>Method</i>	<i>KP-50 weights</i>	<i>KP-50 values</i>	<i>KP-50 capacity</i>	<i>WSMC-10-50</i>
PFL	1.78 ± 0.12	128.55 ± 8.99	7.77 ± 0.50	3.06 ± 0.89
GP-Surrogate	1.04 ± 0.05	75.07 ± 5.20	3.45 ± 0.31	1.18 ± 0.09
SFGE	1.40 ± 0.29	35.40 ± 9.77	4.30 ± 0.67	1.05 ± 0.32
LANCER	4.85 ± 2.53	545.14 ± 233.63	7.20 ± 0.89	3.87 ± 1.78
LODL-MSE	1.76 ± 0.12	127.78 ± 9.36	7.80 ± 8.24	3.04 ± 0.88
LODL-QUADRATIC	2.63 ± 0.34	813.19 ± 108.98	9.34 ± 0.35	5.18 ± 1.14
LODL-DIRECTED-MSE	5.85 ± 0.41	315.08 ± 55.10	17.37 ± 3.97	0.75 ± 0.04
LODL-DIRECTED-QUADRATIC	2.06 ± 0.21	190.34 ± 5.84	14.96 ± 0.41	2.92 ± 0.89
EGL-MSE	1.78 ± 0.09	125.48 ± 6.69	6.41 ± 1.02	2.25 ± 0.32
EGL-QUADRATIC	1.34 ± 0.13	247.49 ± 95.72	6.28 ± 0.33	2.43 ± 0.93
EGL-DIRECTED-MSE	1.75 ± 0.12	129.74 ± 3.76	6.13 ± 0.37	2.32 ± 1.42
EGL-DIRECTED-QUADRATIC	1.97 ± 0.06	275.98 ± 70.70	3.61 ± 0.35	1.36 ± 0.20
SPO	–	13.78 ± 2.82	–	–

E SOLVER CALLS AND RUNTIME COMPARISON

In table 5 we show the average solver calls per instance and the runtime for each baseline model.

810
811
812
813
814
815
816
817
818
819
820
821
822
823
824
825
826
827
828
829
830
831
832
833
834
835
836
837
838
839
840
841
842
843
844
845
846
847
848
849
850
851
852
853
854
855
856
857
858
859
860
861
862
863

F SENSITIVITY ANALYSIS

In table 6 we analyze how β influences results. As expected, higher values lead to an increase in the surrogate loss exploitation. However, we observe a counter-intuitive behavior in average regrets, which improve even if less confident estimations take the place of real regrets. We believe these results may be determined by spurious local optima introduced by the GP loss approximation.

864
865
866
867
868
869
870
871
872
873
874
875
876
877
878
879
880
881
882
883
884
885
886
887
888
889
890
891
892
893
894
895
896
897
898
899
900
901
902
903
904
905
906
907
908
909
910
911
912
913
914
915
916
917

Table 5: Average calls per instance and runtime for all the models on KP-50 with uncertain weights, values and capacity and WSMC-10 with 50 sets.

	<i>Method</i>	<i>KP-50 weights</i>	<i>KP-50 values</i>	<i>KP-50 capacity</i>	<i>WSMC-10-50</i>
<i>S/v. calls</i>	GP-Surrogate	41.33 ± 1.22	42.32 ± 0.09	30.04 ± 0.05	31.06 ± 0.35
	SFGE	304.40 ± 53.80	257.20 ± 34.97	142.60 ± 58.95	358.60 ± 63.62
	LANCER	42.8 ± 3.96	43.2 ± 3.86	30.60 ± 17.24	33.0 ± 22.35
	LODL (ALL)	250.0 ± 0.0	250.0 ± 0.0	250.0 ± 0.0	250.0 ± 0.0
	EGL (ALL)	42.0 ± 0.0	42.0 ± 0.0	32.0 ± 0.0	32.0 ± 0.0
	SPO	–	85.0 ± 6.09	–	–
<i>Runtime</i>	GP-Surrogate	199.40 ± 6.77	136.01 ± 10.02	274.52 ± 66.50	228.73 ± 20.59
	SFGE	717.28 ± 127.26	774.16 ± 173.62	396.93 ± 160.09	1849.74 ± 344.25
	LANCER	207.31 ± 32.24	221.07 ± 20.81	304.38 ± 136.95	348.68 ± 241.32
	LODL (BEST)	365.26 ± 37.76	474.75 ± 35.01	623.06 ± 65.38	1034.88 ± 46.12
	EGL (BEST)	63.01 ± 4.99	72.31 ± 7.40	82.27 ± 3.89	118.99 ± 2.16
	SPO	–	180.51 ± 30.30	–	–

Table 6: Average regret and average calls per instance for GP-Surrogate with different β values on KP-50 with uncertain weights, values and capacity and WSMC-10 with 50 sets.

	<i>Method</i>	<i>KP-50 weights</i>	<i>KP-50 values</i>	<i>KP-50 capacity</i>	<i>WSMC-10-50</i>
<i>Regret</i>	$\beta = 0.01$	1.07 ± 0.14	314.02 ± 263.90	3.76 ± 0.63	5.69 ± 2.17
	$\beta = 0.05$	1.03 ± 0.16	474.31 ± 136.58	3.63 ± 0.32	4.05 ± 1.86
	$\beta = 0.1$	1.01 ± 0.15	176.30 ± 37.33	3.61 ± 0.33	3.87 ± 1.17
	$\beta = 0.5$	1.06 ± 0.12	74.85 ± 4.82	3.57 ± 0.35	1.77 ± 0.43
	$\beta = 1.0$	1.04 ± 0.05	75.07 ± 5.20	3.45 ± 0.31	1.18 ± 0.09
<i>S/v. calls</i>	$\beta = 0.01$	279.16 ± 12.40	148.95 ± 41.43	81.67 ± 21.51	53.65 ± 7.54
	$\beta = 0.05$	156.53 ± 23.56	57.25 ± 3.63	56.84 ± 2.95	71.68 ± 43.56
	$\beta = 0.1$	116.74 ± 13.90	55.52 ± 2.34	41.35 ± 0.84	47.09 ± 2.71
	$\beta = 0.5$	57.75 ± 2.55	40.29 ± 0.30	36.52 ± 0.13	39.73 ± 1.74
	$\beta = 1.0$	41.33 ± 1.22	42.32 ± 0.09	30.04 ± 0.05	31.06 ± 0.35